Trans. of the Society of Instrument and Control Engineers
Vol.E-1, No.1, 116/123 (2001)

Workspace and Manipulability Analysis of Space Manipulator†

Yoji UMETANI* and Kazuya YOSHIDA**

This paper investigates operational performance of space manipulators mounted on a free-floating robot satellite, by defining and analyzing their workspace and manipulability measure.

Since there is no one-to-one correspondence between the joint space and the inertial task space in space free-floating manipulators, a variety of workspaces can be defined according to additional constraints on the motion of the base satellite or on the operational path of the manipulator hand. By specifying such motion, the authors classify and define five types of workspaces, which would be useful to understand the characteristics of a space manipulator.

A new manipulability measure is also defined using the Generalized Jacobian matrix that describes kinematic and dynamic characteristics of a space free-floating manipulator. The manipulability of such a space manipulator is evaluated generally lower than that of ground-based manipulators, reduced by dynamical coupling between the manipulator arm and the base satellite.

Operational posture and configuration design issues are discussed for a two dimensional space robot with respect to wider workspace and higher manipulability.

Key Words: space manipulator, free-floating multi-link system, manipulator performance, workspace, manipulability measure

1. Introduction

A spacecraft system that equips robotic manipulator arms has high potential for future contribution to orbital operation as a telerobotic servicing device. Control issues of satellite mounted arms in such a system have been intensively studied, paying attention to their unique characteristics. [1)~6)].

A main difference of space manipulators from ground-based ones is that the base of the manipulators is not fixed but freely floats and rotates in the orbital environment. We then need a special attention to the dynamic coupling between the arm and the base during the manipulation. Due to this reason, the operational performance of space manipulators becomes reduced from that of the ground-based ones. It is important to understand this mechanism and evaluate how much the manipulator reachability to a target is distorted and the measure of manipulability is degraded for the manipulation in space.

This paper makes qualitative and quantitative analysis on the measures of the workspace and manipulability, both of which are key index to evaluate the performance of a manipulator arm. For space arms, these measures are function of both kinematic parameters such as link length and dynamic parameters such as inertia property. The paper shall provide a useful chart to design and operate a space arm with respect to a better mechanical configuration and a better operational posture.

Table 1 Specification of the system

		Satellite	Manipulator	
		link 0	link 1	link 2
Mass	m_i [kg]	1,000.0	100.0	100.0
Length	ℓ_i [m]	2.6	2.0	2.0
	a_i [m]	1.2	1.0	1.0
	b_i [m]	1.4	1.0	1.0
Inertia	I_i[kgm^2]	635.3	33.3	33.3

2. Modeling

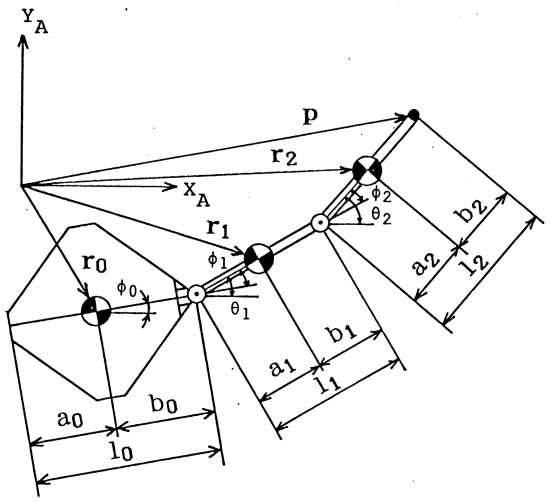

Fig. 1 Model of 2 DOF satellite mounted manipulator

* Toyota Technological Institute
** Tohoku University

2.1 Definitions and Assumptions

For simplicity but not loosing generality, we consider a planer space robotic system that makes a horizontal motion with a 2 DOF manipulator arm. **Fig.1** and **Table 1** illustrate the model configuration and parameter specification. The model comprises three pieces of free-floating rigid bodies connected by two revolute joints. In this section, kinematic relationships for this model are derived.

Mathematical symbols are defined as follows:

$\boldsymbol{r}_i$: a position vector to the centroid of each body with respect to the inertial frame.

$\boldsymbol{p}$: a position vector to the end point of the arm with respect to the inertial frame.

$\boldsymbol{\ell}_i, \boldsymbol{a}_i, \boldsymbol{b}_i$: relative vectors to indicate the link span and its centroid position.

m_i: mass of each link.

I_i: moment of inertia around the centroid of each link.

ω_i: angular velocity around the centroid of each link.

ϕ_0: orientation angle of the satellite base body (link 0).

ϕ_j: rotation angle of each joint.

θ_i: orientation angle of each link with respect to inertia frame ($= \sum_{k=0}^{i} \phi_k$).

Note: $i = 0, 1, 2$ and $j = 1, 2$

The inertial coordinate frame is indicated by Σ_A and the robot coordinate frame, which is fixed on the satellite base body with the origin at joint 1, is indicated by Σ_R All vectors and matrices here are described with respect to the inertial frame unless otherwise specified.

In order to make clear the issues of this paper, the following assumption are made:

(1) The system is composed by rigid bodies.

(2) The motion occurs on the $x-y$ plane, in Fig.1, but no motion in the z direction.

(3) No limitation on joint angles.

(4) In case no position or attitude control of the satellite base, the entire motion of the system is generated only by the joint actuation. In such a case, the conservation of momentum holds true.

2.2 Kinematic Equations

The kinematic equation for the manipulator end point $\boldsymbol{p}$ is derived as follows, in case the origin of Σ_A is located on the centroid of the entire system.

$$\boldsymbol{p} = K_0 \begin{bmatrix} C_0 \\ S_0 \end{bmatrix} + K_1 \begin{bmatrix} C_1 \\ S_1 \end{bmatrix} + K_2 \begin{bmatrix} C_2 \\ S_2 \end{bmatrix} \qquad (1)$$

where

$$\begin{aligned} K_0 &= m_0 b_0 / w \\ K_1 &= (m_0 \ell_1 + m_1 b_1)/w \\ K_2 &= \{(m_0 + m_1)\ell_2 + m_2 b_2\}/w \\ w &= m_0 + m_1 + m_2 \\ C_i &= \cos\theta_i, \quad S_i = \sin\theta_i \end{aligned}$$

By differentiating equation (1) with respect to time, we obtain the following relationship:

$$\begin{aligned} \dot{\boldsymbol{p}} &= \begin{bmatrix} -K_0 S_0 - K_1 S_1 - K_2 S_2 \\ K_0 C_0 + K_1 C_1 + K_2 C_2 \end{bmatrix} \dot{\phi}_0 \\ &\quad + \begin{bmatrix} -K_1 S_1 - K_2 S_2 & -K_2 S_2 \\ K_1 C_1 + K_2 C_2 & K_2 C_2 \end{bmatrix} \begin{bmatrix} \dot{\phi}_1 \\ \dot{\phi}_2 \end{bmatrix} \\ &\equiv \boldsymbol{J}_S \dot{\phi}_0 + \boldsymbol{J}_M \dot{\boldsymbol{\phi}}_M \end{aligned} \qquad (2)$$

This equation describes a basic kinematic relationship among the end point velocity $\dot{\boldsymbol{p}}$, the base angular velocity $\dot{\phi}_0$, and the joint angular velocities $\dot{\boldsymbol{\phi}}_M$.

In a free-floating system without any external control forces or moments, $\dot{\phi}_0$ and $\dot{\boldsymbol{\phi}}_M$ are determined dependently due to the internal coupling, and this coupling effect is modeled by the momentum conservation law.

The conservation equations for linear momentum and angular momentum are expressed as follows, respectively:

$$\sum_{i=0}^{2} m_i \dot{\boldsymbol{r}}_i = const. \qquad (3)$$

$$\sum_{i=0}^{2} (\boldsymbol{I}_i \dot{\boldsymbol{\theta}}_i + m_i \boldsymbol{r}_i \times \dot{\boldsymbol{r}}_i) = const. \qquad (4)$$

Equation (3) is time integrable and yields a kinematic equation about mass centroid (1). On the other hand, the integral of equation (4) is not uniquely determined but depends on the manipulator motion paths, and hence Equation (4) gives a non-holonomic constraint to the system. By solving Equation (3) for $\dot{\boldsymbol{r}}_i$, then substituting it into (4), we obtain the following equation about angular velocities:

$$I_S \dot{\phi}_0 + \boldsymbol{I}_M \dot{\boldsymbol{\phi}}_M = 0 \qquad (5)$$

Here zero initial momentum is assumed. The matrices I_S and $\boldsymbol{I}_M$ are the moment of inertia corresponding to $\dot{\phi}_0$ and $\dot{\boldsymbol{\phi}}_M$, respectively.

Equations (2) and (5) form a set of simultaneous linear equation for $\dot{\phi}_0$ and $\dot{\boldsymbol{\phi}}_M$. By solving (5) for $\dot{\phi}_0$ and substituting into (2), we obtain the expression for the end point velocity $\dot{\boldsymbol{p}}$ as a direct function of joint angular velocity $\dot{\boldsymbol{\phi}}_M$, by canceling out the base variables:

$$\begin{aligned} \boldsymbol{J} &= (\boldsymbol{J}_M - \boldsymbol{J}_S \boldsymbol{I}_M / I_S) \dot{\boldsymbol{\phi}}_M \\ &\equiv \boldsymbol{J}^* \dot{\boldsymbol{\phi}}_M \end{aligned} \qquad (6)$$

Equation (6) describes the kinematic and dynamic relationship of the space manipulator mounted on a free-floating base, in the same format as a conventional kine-

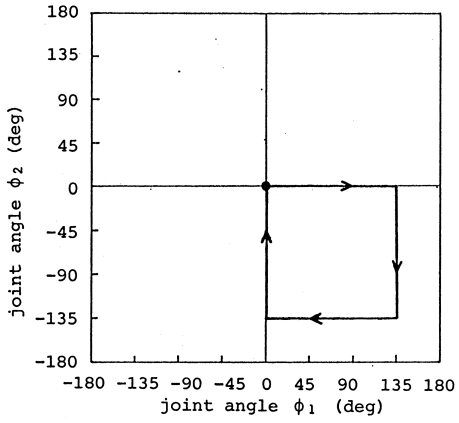

(a) cyclic operation in joint space

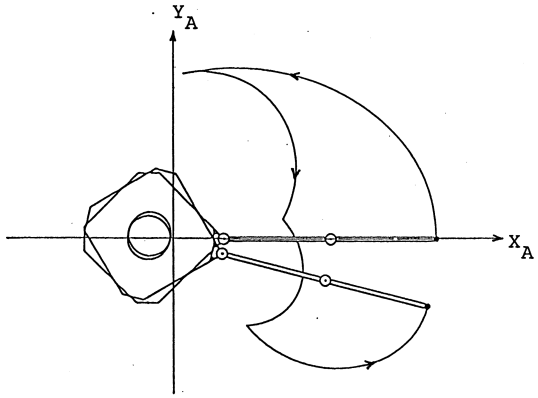

(b) course of postural change

Fig. 2 Satellite attitude change by a cyclic manipulator operation

matic equation for ground-based manipulators. The matrix $\boldsymbol{J}^*$ (a 2 by 2 square matrix here) is called "Generalized Jacobian matrix" for space free-floating manipulators [5].

3. Workspace Analysis

3.1 Definition of Workspaces

In this section, reachable workspaces of a space manipulator are discussed.

In case of no external forces or moments on a space free-floating robot, the state of the system depends on its motion history and there is no closed form solution for inverse kinematics problems. For example, when a 2 DOF space manipulator is operated in a cyclic motion sequence in the joint space as depicted in **Fig.2** (a), the course of postural change of the system is computed by equations (1) and (5) to yield Fig.2 (b). The end point positions of the arm become different in the inertial space, although the joint angles are the same between the before and after the motion. This evidences that there is no one-to-one correspondences between the joint space and the inertial task space, then infers that the kinematic reachability of the arm in the inertial space cannot be discussed only by joint angles, but the consideration to their motion trace or other motion constraints is necessary.

Vafa and Dubowsky [3] pointed out three fundamental cases to discuss the workspace with respect to the condition of the base satellite: (1) the orientation and the position of the base is constraint, (2) only the orientation is constraint, and (3) no constraint on the base. This paper follows their idea and elaborate the last case into three sub cases, then proposes five cases of workspaces in total. They are defined as follows:

(1) Fixed Vehicle Workspace

Fixed Vehicle Workspace is a reachable envelope of the manipulator end point in case the orientation and position of the base satellite (vehicle) are fixed. Such situation can be achieved by the control with reaction wheels and gas jet thrusters mounted on the base, so that the space manipulator shall behave in the same way as ground based manipulators. In this case, the workspace is in a circle with radius $L = \ell_1 + \ell_2$, centered at the manipulator attachment point (joint 1), or the origin of Σ_R.

(2) Attitude Constraint Workspace

Attitude Constrain Workspace is a reachable envelope in case only the orientation of the base satellite (vehicle) is fixed. Such condition is given with $\phi_0 = const.$ and a maximum reach is obtained at $\phi_2 = 0$. By putting $\phi_0 = \phi_2 = 0$ in equation (1), we obtain the following expression for the end point position $\boldsymbol{p}$:

$$\boldsymbol{p} = \begin{bmatrix} K_0 \\ 0 \end{bmatrix} + (K_1 + K_2) \begin{bmatrix} \cos\phi_1 \\ \sin\phi_1 \end{bmatrix} \tag{7}$$

This equation represents a circle with radius $K_1 + K_2$, centered at $(K_0, 0)$ in the inertial frame.

In this case, the robot frame keeps a constant orientation but the position of its origin changes due to the manipulator reaction.

(3) Free Workspace

In case of no constraint on the base satellite, the manipulator workspace depends on its motion path. Here, three types of workspaces are defined with respect to the motion specification of the arm.

(3-a) Maximum Reachable Space

If we do not specify the path of the manipulator arm, equation (1) can take arbitrary values on ϕ_0, ϕ_1 and ϕ_2, noting that a cyclic motion path can change the base orientation ϕ_0. Therefore the manipulator end point can reach any point inside a circle with radius $K_0 + K_1 + K_2$,

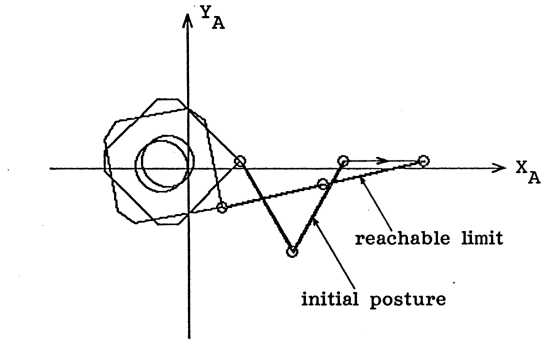

(a) straight-path tracking to the reachable limit

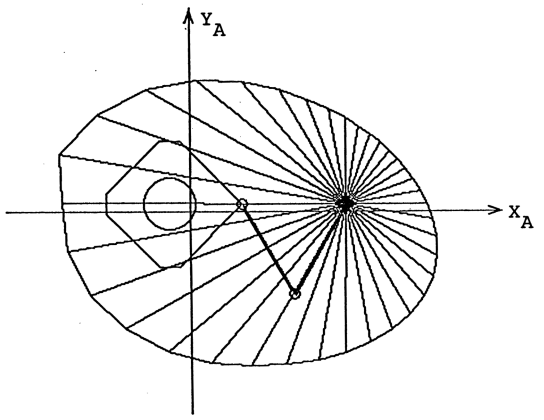

(b) calculated reachable limits to all directions

Fig. 3 Straight-path workspace

centered at $(0, 0)$ in the inertial frame. This area is named *Maximum Reachable Space.*

(3-b) Straight-Path Workspace

As a typical motion constraint of the arm, straight paths of the end point are considered. A reachable limit of the straight path approach is given by kinematic singularity at $\phi_2 = 0$ in the joint space. However, as the orientation of the base changes along the manipulator motion, it is difficult to obtain an algebraic expression to describe such a limit in the inertial space. Here a numerical method is employed to illustrate the straight-path reachable limit from a given initial point to all possible motion directions.

Fig.3 shows an example of such limits from an initial posture at $\phi_0 = 0$ [deg], $\phi_1 = -60$ [deg], and $\phi_2 = 120$ [deg]. Fig.3 (a) depicts a single path from the initial posture to a reachable limit in the X_A direction. This is obtained by numerical simulation using the inversion of equation (6). By checking the limits for all directions in this way, *Straight-Path Workspace* for the given initial posture is obtained as Fig.3 (b)

(3-c) Guaranteed Workspace

Finally, a workspace within which the accessibility is always guaranteed from arbitrary initial postures and with arbitrary approaching paths, is considered.

A common area, or union, of the Straight-Path Workspaces with various initial postures forms a circular workspace, to which the hand is accessible from arbitrary initial postures. An expression for such a circle is obtained as follows. The boundary of the Straight-Path Workspaces is given by the manipulator singularity at $\phi_2 = 0$. Substituting $\phi_2 = 0$ into equation (1), we obtain:

$$\boldsymbol{p} = K_0 \begin{bmatrix} \cos\phi_0 \\ \sin\phi_0 \end{bmatrix} + (K_1 + K_2) \begin{bmatrix} \cos(\phi_0 + \phi_1) \\ \sin(\phi_0 + \phi_1) \end{bmatrix}$$

Among the solution for $\boldsymbol{p}$, the minimum reach (shortest distance) from the system centroid is given at $\phi_1 = \pm\pi$, and with this condition, the equation becomes as:

$$\boldsymbol{p} = \{K_0 - (K_1 + K_2)\} \begin{bmatrix} \cos\phi_0 \\ \sin\phi_0 \end{bmatrix} \tag{8}$$

This equation represents a circle with radius $|K_0 - (K_1 + K_2)|$, centered at $(0, 0)$ in the inertial frame. This area is termed *Guaranteed Workspace.* In this workspace, the manipulator motion is free from the singularity of $\phi_2 = 0$, then the accessibility is guaranteed from arbitrary initial postures and with arbitrary motion paths.

Vafa and Dubowsky called this particular workspace as Free Workspace [3]. But as discussed here, the Free Workspace, in the sense that the base is free, is not unique but defined into three typical cases depending on the motion path of the arm. Here the present authors propose to redefine Vafa and Dubowsky's Free Workspace as *Guaranteed Workspace* to clarify its meaning.

3. 2 Relationship Among Workspaces

Fig.4 depicts the relationship of four of workspaces defined above, Area 1: Fixed-Vehicle Workspace, Area 2: Attitude Constraint Workspace, Area 3: Maximum Reachable Space, and Area 5: Guaranteed Workspace. Among them, the relationship

Area 3 $\supseteq$ Area 2 $\supseteq$ Area 5

holds always true, and with an additional condition:

$$b_0 \geq \frac{w}{m_0}(L - K_1 - K_2), \tag{9}$$

another relationship

Area 3 $\supseteq$ Area 1 $\supseteq$ Area 2

becomes also true.

Fig.5 depicts the relationship of three Free Workspaces, Area 3: Maximum Reachable Space, Area 4: Straight-Path Workspace and Area 5: Guaranteed Workspace.

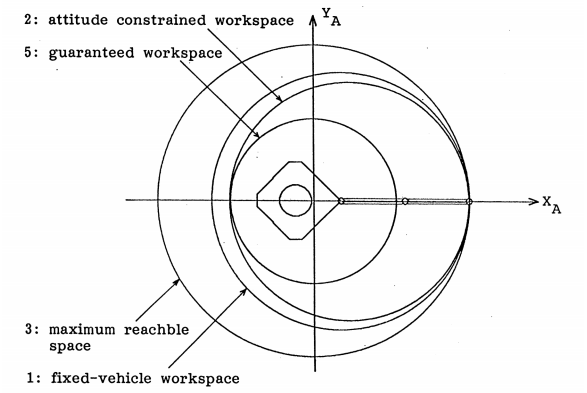

Fig. 4 Relationship of workspaces

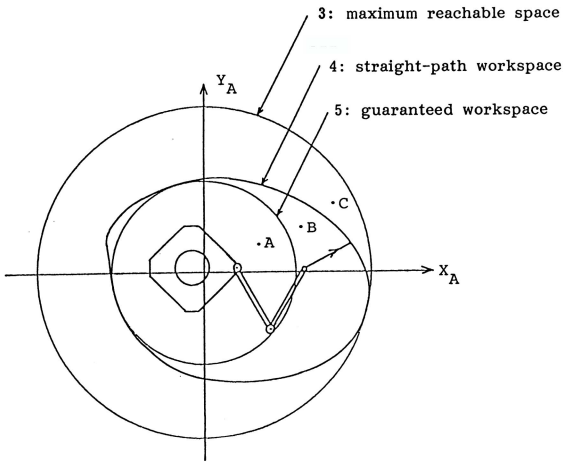

Fig. 5 Relationship of free workspace

Area 3 is a union of Area 4 with various initial postures. Area 5 is an intersection of Area 4 with various initial postures. Point A is characterized as a point to which the accessibility is guaranteed from arbitrary initial postures via arbitrary paths. Point B is characterized as a point which can be accessed from the depicted initial posture via a straight-line path. Point C is characterized as a point which cannot be accessed from the depicted initial posture via a straight-line path, but can be reached after reorienting the base by a suitable cyclic maneuver.

In the above discussions, it is assumed no limitation on the joint angles. In practical cases with joint angle limitations, the workspaces become subsets of the areas defined and discussed above.

4. Manipulability Analysis

4.1 Definition of Manipulability Measure for Space Manipulator

In this section, a new manipulability measure for space manipulator is defined. As a performance index of a manipulator arm, the concepts called Manipulability Measure and Manipulability Ellipsoid are defined based on the singular value analysis of the manipulator Jacobian matrix [7) 8)].

Here the same methodology is applied to define those concepts for a space manipulator using the Generalized Jacobian Matrix $\boldsymbol{J}^*$, given in equation (6). The manipulability measure of a space free-floating manipulator w^* is defined as:

$$w^* = \sqrt{\det\{[\boldsymbol{J}^*][\boldsymbol{J}^*]^{\mathrm{T}}\}} \tag{10}$$

A set of possible end tip motion $\dot{\boldsymbol{p}}$ corresponding to the confined joint motion by $\|\dot{\boldsymbol{\phi}}_M\| \leq 1$ form an ellipsoid in n dimensional space (n is the number of DOF of the hand.) The length of principle axes of the ellipsoid is given by the singular values of matrix $\boldsymbol{J}^*$ and the volume of the ellipsoid is in proportion to w^*.

Since the Generalized Jacobian Matrix $\boldsymbol{J}^*$ is not a simple kinematic function but involves dynamic properties such as mass and moment of inertia of the base and the arm, as its derivation is described in equations (2)(5)(6), the manipulability measure for space manipulator w^* is also the function of both kinematic and dynamic property of the robot.

4.2 Manipulability Analysis for Space Manipulator

Fig.6 depicts a Manipulability Ellipsoids for a space manipulator specified in Fig.1 and Table 1. There are two configurations, elbow-down and elbow-up, to reach a given point and here the elbow-down ($\phi_2 \geq 0$) cases are considered. As discussed in the previous section, there is no one-to-one correspondence between the robot posture and inertial end tip position, then the Manipulability Measures and Ellipsoids are displayed in the robot fixed coordinate frame Σ_R.

The distribution of the Manipulability Measure is displayed by a contour map in **Fig.7** (a). For comparison, a contour map of the manipulability for a ground-based manipulator is depicted in Fig.7 (b). Index numbers written on the figures are normalized value of the manipulability measure by:

$$\hat{w}^* = w^*/L^n \qquad (\text{here } n = 2.) \tag{11}$$

The numbers are multiplied by 40 to be marked in the figures.

From these figures, it is clearly seen that the manipulability measure of a space free-floating manipulator is generally lower than that of a ground-fixed manipulator. This is because the manipulability is degraded by the base motion due to the manipulator reaction. Looking at the

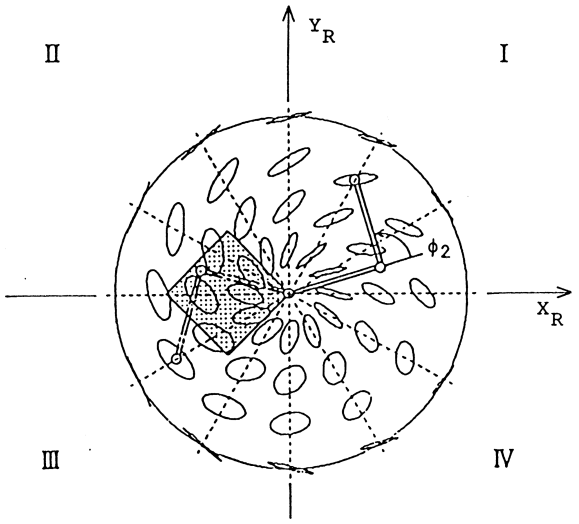

Fig. 6 Manipulability ellipsoids for a 2-link space manipulator

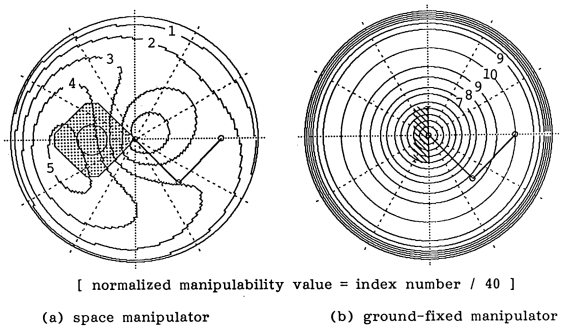

Fig. 7 Contour maps of manipulability measure

distribution of the manipulability measure, the space arm has non-circular, non-symmetric counter lines, while the ground arm does concentric-circular counter lines. Particularly, the manipulability measure shows relatively lower values in the first quadrant of the robot coordinate frame and relatively better in the third quadrant. This is because the manipulator reaction effect is more significant when the arm is reached out in front of the robot, but less significant when the arm is retracted to work on and behind the robot base.

Here, an illustrative example is given to show the posture dependency of the manipulability due to the reaction effect. **Fig.8** (a) and (b) show two different postures to reach the same end tip position. Posture 1 is an elbow-down configuration corresponding to the first quadrant case of Figs.6 and 7. Posture 2 is an elbow-up configuration, which is equivalent to the case where the end tip is located in the fourth quadrant in Fig.6 and 7. The obtained manipulability ellipsoids become different between the two postures.

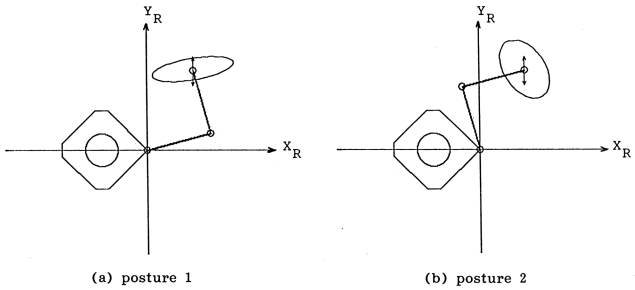

Fig. 8 Manipulability ellipsoids for different postures

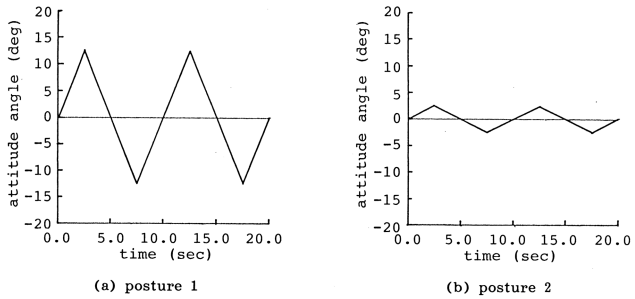

Fig. 9 Satellite attitude change according to the same tip motion in the different postures

Now, let us consider small go-and-back motion of end tip in the Y_R direction. As seen from posture 1 of Fig.8, the given motion direction almost coincides with the direction of minimum axis of the ellipsoid. The minimum axis of ellipsoid means minimum manipulability of the hand and maximum reaction on the base for the given operation. On the other hand, in posture 2, the ellipsoid is relatively roundish then has longer intersection in the direction of the end tip motion. This suggests higher manipulability measure and smaller reaction.

The above comments are evidenced by simulations for the base attitude reaction, as shown in **Fig.9.** The same go-and-back motion is given at the end tip although, the base reaction becomes very different between the postures 1 and 2. The posture 1 has a lower performance of the end tip motion to the given direction and bigger reaction effect on the base. Yet, the posture 2 has higher end tip performance and lower reaction effect. The latter case is better from this specified operation.

The manipulability measure for a space manipulator is under strong influence of the base reaction, then its evaluation is useful to understand not only the performance of the end-tip motion but also the attitude disturbance of the base due to the manipulator reaction.

Table 2 Normalized average manipulability measure $\bar{\bar{w}}^*$ and normalized work areas $\hat{S}_M, \hat{S}_G$.

b_0/B_0	$\bar{\bar{w}}^*[\times 10^{-2}]$	$\hat{S}_M$	$\hat{S}_G$
0	5.59	0.84	0.84
0.5	5.93	1.13	0.59
1.0	6.70	1.46	0.39
1.5	7.52	1.83	0.23
2.0	8.08	2.25	0.11

5. Application to Design Issues

In this section, the performance evaluation by the workspace volume (area) and manipulability measure is applied to a design issue of a space robot.

As an illustrative example, a discussion is made to decide the attachment point of a manipulator arm in a 2 DOF planar system as shown in Fig.1. Here, we try to change the distance from the base centroid and joint 1, b_0, while holding other parameters as listed in Table 1. The value of b_0 in Table 1 is 1.4 [m] and set it as B_0, then $b_0 = 0$ means the arm shall be attached on the base centroid, $b_0/B_0 = 1$ is the case same as Fig.1, and $b_0/B_0 > 1$ indicates cases the arm shall be mounted at the end of a massless bar, sticking out of the base.

The evaluation is made with three indices: (1) the area of Maximum Reachable Space, $\hat{S}_M$, and (2) the area of Guaranteed Workspace, $\hat{S}_G$, both are normalized by πL^2, and (3) the manipulability measure averaged the reachable area in the robot coordinate frame:

$$\bar{\bar{w}} = \int \hat{w}^* ds / \int ds \tag{12}$$

(where ds is an infinitesimal area on the robot frame.)

The result of the evaluation is listed in **Table 2** and typical three cases at $b_0/B_0 = 0, 1, 0, 2, 0$ are depicted in **Fig.10**. The result shows that the area $\hat{S}_M$ and the manipulability $\bar{\bar{w}}$ increase, on the other hand, the area $\hat{S}_G$ decreases, according to the increment of the length b_0. The reason for the increment of $\bar{\bar{w}}$ is understood that the moment of the inertia of the base increases for longer b_0, then the robot base receives smaller effect from the manipulator reaction.

From the view point of the space robot design with higher performance, it is desirable to have wider guaranteed workspace and higher manipulability. However, the result shows that these two yield contradictory criteria. Particularly, longer b_0 is effective to increase the manipulability but limits the Guaranteed Workspace to close vicinity of the base.

Here, an important consequence is that the operational performance is greatly influenced just by changing the attachment point of the manipulator arm. Careful trade-off

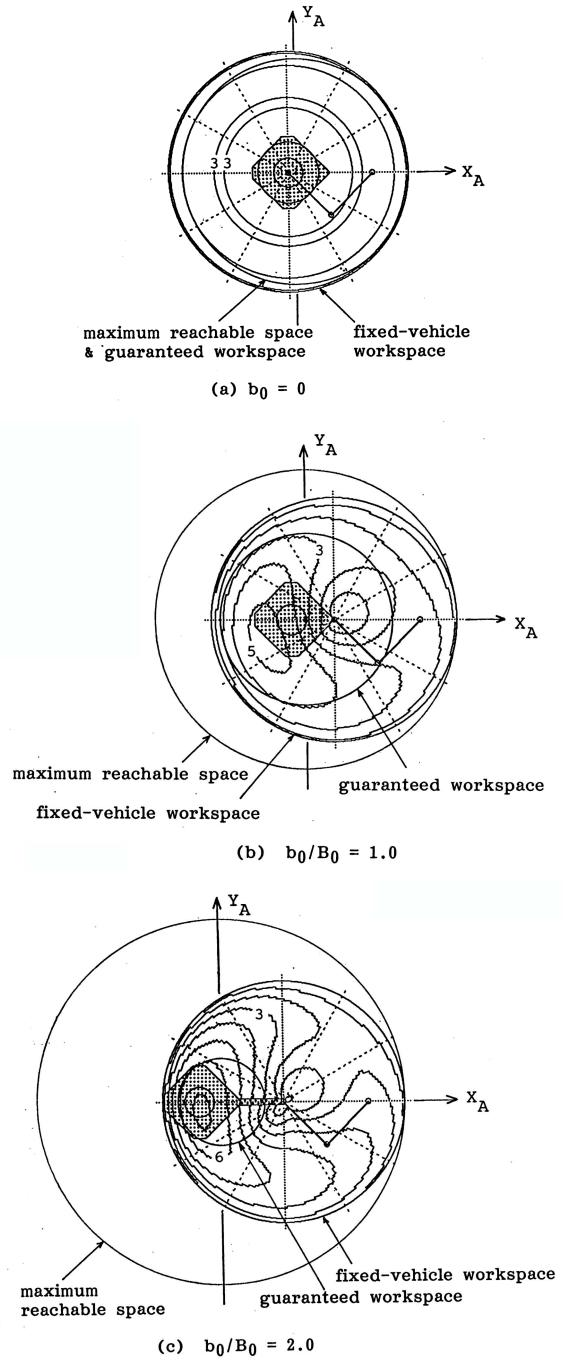

Fig. 10 Workspace and manipulability distributions for different space robot configurations

is therefore necessary to design a practical system with respect to the workspace area and manipulability measure, which are function of not only kinematics but also inertia property of the entire system.

6. Conclusions

In this paper, the measures of workspace and manipulability for a free-floating space robot are discussed.

First, it is pointed out that the workspace should be defined with various conditions on the motion of the base satellite or the operational path of the manipulator hand. According to these conditions, the authors define five types of workspaces. They are all important but, of particular, two concepts named *Maximum Reachable Space* and *Guaranteed Workspace* are useful to characterize the performance of the free-floating manipulator.

Next, the measure of the manipulability is defined using the Generalized Jacobian matrix. It is clarified that the manipulability measure of space manipulator is degraded in non-isometric way due to the dynamic coupling of the arm and base.

Finally, the design issue of a space robot is discussed with an illustrative example to determine the position to attach the shoulder joint. The performance of each design is evaluated by Maximum Reachable Space, Guaranteed Workspace, and Manipulability Measure. These indices show contradictory evaluation versus the parameter b_0/B_0, the normalized distance of the attachment point. It is suggested that a careful trade-off is necessary for the design of a practical system. However, an important note is made here that the operational characteristics is not determined just by kinematic conditions, but also dynamic conditions such as inertia property of the entire system.

The authors express their special thanks to Mr. Mitsuaki Fujimori, who was with the authors at Tokyo Institute of Technology as a graduate student and currently with Yokogawa Electric Corporation, for his contribution to make the contour maps of the manipulability measure.

References

1) K. Yamada, K. Tsuchiya and T. Tadakawa: Modeling and Control of a Space Manipulator, Proc. 13th Int. Symp. Space Technol. Sci. 1982, 993/998 (1982)
2) R. W. Longman, R. E. Lindberg and M. F. Zedd: Satellite-Mounted Robot Manipulators - New Kinematics and Reaction Moment Compensation, Int. J. Robotics Research, 6-3, 87/113 (1987)
3) Z. Vafa and S. Dubowsky: On the Dynamics of Manipulators in Space Using the Virtual Manipulator Approach, Proc. 1987 IEEE Int. Conf. Robotics and Automation, 597/585 (1987)
4) H. L. Alexander and R. H. Cannon, Jr.: Experiments on the Control of a Satellite Manipulator, Paper at 1987 IEEE American Control Conf., 1/10 (1987)
5) Y. Umetani and K. Yoshida: Continuous Path Control of Space Manipulators Mounted on OMV, Acta Astronautica, 15-12, 981/986 (1987)
6) Y. Masutani, F. Miyazaki and S. Arimoto: Sensory Feedback Control for Space Manipulators, Proc. 1989 IEEE Int. Conf. Robotics and Automation, 1346/1351 (1989)
7) T. Yoshikawa: Measure of Manipulatability for Robot Manipulators, J. of Robotics Society of Japan, 2-1, 63/67 (1984) (in Japanese)
8) M. Uchiyama, K. Shimizu and K. Hakomori: Performance Evaluation of Robotic Arms Using the Jacobian, Trans. of the Society of Instrument and Control Engineers, 21-2, 82/88 (1985) (in Japanese)

Reprinted from Trans. of the SICE
Vol. 26 No. 2 188/195 1990

Yoji Umetani

Dr. Umetani received B. Eng. degree in 1956 from Kyoto University, Japan, and Dr. Eng. degree in 1969 from Tokyo Institude of Technology, Japan.

From 1959 to 1970, he was with the Research Institute on Industrial Science, University of Tokyo, as a Lecturer. In 1970, he became as Associate Professor, in 1975 a Professor, and 1990 Dean of the Faculty of Engineering, Tokyo Institute of Technology. Since 1993, he has been a Professor in the Graduate School of Engineering, Toyota Technological Institute, Japan.

His research field covers very broad over system dynamics and control, bioengineering approach to mobile robots, optimal shape design, space robotics, and human-robot co-existence problems. He received a lot of awards including J. F. Engelberger Award in 1991.

Kazuya Yoshida

Dr. Yoshida received B. Eng., M. Eng., and Dr. Eng. degrees in 1984, 1986, and 1990, respectively, from Tokyo Institute of Technology, Japan.

From 1986 to 1994, he was a Research Associate in Tokyo Institute of Technology. In 1994, he was with Massachusetts Institute of Technology, U. S. A. as a Visiting Scientist. Since 1995, he has been an Associate Professor in the Graduate School of Engineering, Tohoku University, Japan. Since 1998, he also serve as a Visiting Lecturer in International Space University.

His research field covers space robotics, particularly kinematics, dynamics and control issues of space manipulators in orbit as well as robotic systems for planetary exploration. He has been involved in a number of national space projects He received a lot of awards including the IEEE Best Conference Paper Award in 2001.